Genome-Wide Studies Reveal That Lin28 Enhances the Translation of Genes Important for Growth and Survival of Human Embryonic Stem Cells

SHUPING PENG,[a,b]* LING-LING CHEN,[c] XIN-XIANG LEI,[a,d] LI YANG,[c] HAIFAN LIN,[b] GORDON G. CARMICHAEL,[c] YINGQUN HUANG[a,b]

[a]Department of Obstetrics, Gynecology and Reproductive Sciences, Yale University School of Medicine, New Haven, Connecticut, USA; [b]Yale Stem Cell Center, Yale University School of Medicine, New Haven, Connecticut, USA; [c]Department of Genetics and Developmental Biology, University of Connecticut Stem Cell Institute, University of Connecticut Health Center, Farmington, Connecticut, USA; [d]Department of Chemistry, Wenzhou University, Zhejiang, People's Republic of China

ABSTRACT

Lin28 inhibits the expression of let-7 microRNAs but also exhibits let-7-independent functions. Using immunoprecipitation and deep sequencing, we show here that Lin28 preferentially associates with a small subset of cellular mRNAs. Of particular interest are those for ribosomal proteins and metabolic enzymes, the expression levels of which are known to be coupled to cell growth and survival. Polysome profiling and reporter analyses suggest that Lin28 stimulates the translation of many or most of these targets. Moreover, Lin28-responsive elements were found within the coding regions of all target genes tested. Finally, a mutant Lin28 that still binds RNA but fails to interact with RNA helicase A (RHA), acts as a dominant-negative inhibitor of Lin28-dependent stimulation of translation. We suggest that Lin28, working in concert with RHA, enhances the translation of genes important for the growth and survival of human embryonic stem cells. STEM CELLS 2011;29:496–504

Disclosure of potential conflicts of interest is found at the end of this article.

INTRODUCTION

Highly expressed in human embryonic stem cells (hESCs), Lin28 facilitates the reprogramming of fibroblasts to induced pluripotent stem cells (iPSCs) by increasing the number of reprogrammed clones [1]. This is consistent with a role for Lin28 in cell growth and survival. Also consistent is the recent report that Lin28 knockout mice were severely underdeveloped and nonviable [2]. These effects likely result from several distinct molecular functions. Lin28 inhibits the biogenesis of a group of microRNAs, among which are the let-7 family microRNAs shown to participate in the regulation of expression of genes involved in cell growth and differentiation [3, 4]. This protein binds to the loop regions of microRNA precursors and blocks their processing into mature microRNAs [5–7]. In addition, Lin28 induces uridylation of the precursors and promotes their degradation [8–10]. On the other hand, Lin28 alters cell fates during neurogliogenesis via mechanisms distinct from those mediated by let-7 and causes changes in gene expression before any effect on let-7 could be detected [11]. Likewise, a mutant Lin28 that permits let-7 production could still completely inhibit gliogenesis [11]. Moreover, Zhu et al. [2] have recently demonstrated that transgenic mice that overexpress Lin28 exhibit overgrowth and delayed onset of puberty. However, no decrease in the level of let-7 was observed in the hypothalamic-pituitary-gonadal axis that plays a critical role in controlling development and reproduction. Therefore, mechanisms other than let-7-mediated pathways must also play important roles in Lin28-dependent gene regulation. During muscle cell differentiation, Lin28 binds to insulin-like growth factor (IGF)-2 mRNA and stimulates its translation [12]. It also selectively binds to mRNAs of the key pluripotency factor Oct4 and a subset of cell cycle-related factors and promotes their expression at the post-transcriptional level [13–15]. Lin28-responsive elements (LREs) have been mapped to the 5′-, 3′-untranslated regions, or open reading frames (ORFs) of mRNA targets [12–15]. Recently, post-transcriptional

regulation mediated by Lin28 has been shown to require a functional interaction with RNA helicase A (RHA) [15].

MATERIALS AND METHODS

Antibodies, siRNAs, and Plasmids

The antibodies specific for high mobility group AT-hook1 (HMGA1) (Santa Cruz, sc-8982; Santa Cruz, CA, http://www.scbt.com/index.html), CD63 (Santa Cruz, sc-15363), ribosomal protein S13 (RPS13) (Protein Tech Group Inc., 16680-1-AP; Chicago, IL, http://www.ptglab.com/), eukaryotic translation elongation factor 1 gamma (EEF1G; Abcam, ab72368; Cambridge, MA, http://www.abcam.com/), Lin28 (Abcam, ab46020), Oct4 (Santa Cruz, sc-5279), RHA (Abcam, ab54593), β-tubulin (Abcam, ab6046), β-actin (Abcam, ab8226), Flag (Santa Cruz, sc-807; Stratagene, 200472; Santa Clara, CA, www.stratagene.com), and rabbit pre-immune serum (SouthernBiotech, 0040-01; Birmingham, AL, www.southernbiotech.com) were purchased. The siLin28 (Dharmacon, ON-TARGETplus SMARTpool, L-018411-01; Lafayette, Colorado, www.dharmacon.com), siLin28-2 (an equal molar mixture of two siRNAs, J-018411-09 and J-018411-11), siCon (Dharmacon, D-001810-10-05), and the plasmid-expressing Flag-Lin28 were previously described [15]. Flag-Lin28ΔC was created by cloning a PCR fragment containing part of the human Lin28 coding region (aa 1–176, relative to the translational start site) into pFLAG-CMV-2 (Sigma, E7398) at the NotI and BamHI sites. The luciferase reporter constructs Oct4-R2, Oct4-R4 [15], and H2a [14] were previously documented. Constructs Oct4-95 (Gene ID: NM_002701), HMGA1-ORF (Gene ID: NM_002131), RPS13-ORF (Gene ID: NM_001017), EEF1G-R3 (Gene ID: NM_001404), and Oct4-70 (Gene ID: NM_002701) were made by inserting PCR fragments containing nucleotides 516–610, 323–613, 33–488, 811–1,140, and 541–610 (relative to the transcriptional start sites) of the corresponding genes, respectively, at the NotI and XhoI sites of the firefly reporter vector [14].

Cell Culture and Transfection

The culture and transfection of the hESC line H1 (WA01, WiCell), embryonal carcinoma (EC) line PA-1, and HEK293 cells were carried out as preciously described [15].

Protein Extraction and Western Blot Analysis

These were carried out as described in [15].

Ribonucleoprotein Particle Immunoprecipitation and RT-qPCR

Ribonucleoprotein particle (RNP) immunoprecipitation (IP) experiments were carried out essentially as described [15]. To prepare samples for deep sequencing, IP was scaled up 10-fold. The real-time PCR primers are listed below. β-actin forward: 5′-ATCAAGATCATTGCTCCTCCTGAG; β-actin reverse: 5′-CTG CTTGCTGATCCACATCTG; β-tubulin forward: 5′-CGTGTTCG GCCAGAGTGGTGC; β-tubulin reverse: 5′-GGGTGAGGGCAT GACGCTGAA; Lin28 forward: 5′-CGGGCATCTGTAAGTGGT TC; Lin28 reverse: 5′-CAGACCCTTGGCTGACTTCT; Oct4 forward: 5′-GTGGAGGAAGCTGACAACAA; Oct4 reverse: 5′- GC CGGTTACAGAACCACACT; firefly luciferase forward: 5′-GCT GGGCGTTAATCAGAGAG; firefly luciferase reverse: 5′-GTG TTCGTCTTCGTCCCAGT; *Renilla* forward: 5′-GCAAATCAGG CAAATCTGGT; *Renilla* reverse: 5′-GGCCGACAAAAATGATC TTC; HMGA1 forward: 5′-CAGCGAAGTGCCAACACCTAAG; HMGA1 reverse: 5′-CCTTGGTTTCCTTCCTGGAGTT; RPS13 forward: 5′-CTCTCCTTTCGTTGCCTGAT; RPS13 reverse: 5′CCCTTCTTGGCCAGTTTGTA; eukaryotic translation initiation factor 4A (EIF4A) forward: 5′-TGCTTAACCGGAGATAC CTGTC; EIF4A reverse: 5′-GTCCCTCATGAACTTCTTGGTC;

CD63 forward: 5′-CCCGAAAAACAACCACACTGC; CD63 reverse: 5′-GATGAGGAGGCTGAGGAGACC; EEF1G forward: 5′- AGCGGAAGGAGGAGAAAAAG; EEF1G reverse: 5′-GACC AGCCGTCCTTATCAAA.

Deep Sequencing Analysis

Lin28 and preimmune IP RNA samples from H1 cells were used for deep sequencing analysis, and the sequencing libraries were prepared according to the manufacturer's instructions (Illumina, P/N 1004814; San Diego, CA, http://www.illumina.com/applications.ilmn). Briefly, RNAs extracted from IP samples were treated by two successive rounds of oligo-dT selection. The poly(A)$^+$ RNAs were fragmented using divalent cations under elevated temperature, followed by first and second strand cDNA synthesis with random hexamer priming. The cDNA fragments were cleaned up, end-repaired, and phosphorylated at their 5′ ends. After a nontemplated 3′ end addition of A residues, Illumina adapters were ligated to both ends, and ∼300-bp fragments were isolated and amplified by PCR using Illumina adapters. The libraries derived from Lin28 IP and preimmune IP samples were individually used for sequencing on an Illumina GAII platform using a single-read protocol. Approximately 10 million reads were obtained from each IP sample, and these sequences were aligned to the human genome using Bowtie [16]. For both preimmune and Lin28 IP libraries, ∼4.7 to ∼6.0 million reads were uniquely aligned. The sequencing reads were uniquely aligned to the human hg18 genome and splice junction index using Bowtie [16] that allows up to two mismatches. Wiggle track files were generated from Bowtie output files by a custom bowtie2wiggle script and loaded onto the UCSC genome browser (2006; http://www.genome.ucsc.edu) for visualization. Gene expression levels were determined by calculating quantitative RPKM scores (Reads Per Kilobase of gene model per Million mapped reads) as described [17]. The raw data can be accessed at http://www.ncbi.nlm.nih.gov/geo/query/acc.cgi?token=nrktvaqeewuiyrs&acc=GSE23109. mRNAs that were enriched by at least 2.5-fold in the Lin28 IP compared with preimmune were selected as significant Lin28 targets.

Gene Ontology Analysis. Gene ontology (GO) terms of Lin28 IP mRNA targets were identified using the Funcassociate 2.0 software [18], where these mRNAs were used as the "query" set and all human genes as the "gene space" set.

Sucrose Gradient Polysome Fractionation

These were carried out essentially as described previously [15]. Briefly, PA-1 cells (3×10^7) were harvested, washed with PBS, and resuspended in 0.5 ml of freshly prepared extraction buffer (100 mM KCl, 0.1% TritonX-100, 50 mM 4-(2-hydroxyethyl)-1-piperazineethanesulfonic acid (HEPES), pH 7.4, 2 mM MgCl$_2$, 10% glycerol, 1 mM dithiothreitol (DTT), 20 U/ml Protector RNase [Roche], 1× complete mini EDTA-free protease inhibitor cocktail [Roche]). After incubation on ice for 10 minutes, the lysate was centrifuged at 1,300g at 4°C for 10 minutes to remove insoluble materials. The supernatant was applied onto the top of a 15%–55% (wt./wt.) linear sucrose gradient and centrifuged at 150,000 g for 3 hours in a Beckman ultracentrifuge. Fractions (0.2 ml each) were collected and used for RNA extraction or protein analysis. In the case of polysome IP, pooled polysome fractions in a total of ∼4 ml were divided into two tubes and incubated with protein A sepharose beads prebound with either anti-Lin28 antibody or preimmune IgG at 4°C overnight. Bound RNAs were extracted and used in reverse transcription and quantitative polymerase chain reaction (RT-qPCR) analysis.

Luciferase Assays

These were carried out basically as previously described [13]. Briefly, the indicated firefly luciferase reporter plasmids were each transfected into HEK293 cells, with or without cotransfection of Flag-Lin28 or Flag-Lin28ΔC. The *Renilla* reporter was

included in all transfections for normalization purposes. Transfection was carried out in a 48-well plate scale. The amount of total plasmid DNA per well was 400 ng that included 100 ng of firefly luciferase reporter, 2 ng of *Renilla*, and the indicated amounts of Flag-Lin28 or Flag-Lin28ΔC.

Coimmunoprecipitation

To examine the interaction between Flag-Lin28 (or Flag-Lin28ΔC) with RHA, 8×10^6 HEK293 cells were transfected with 6 μg of Flag-Lin28, Flag-Lin28ΔC, or empty vector in a 6-cm plate scale. Cells were collected 48 hours later by manual scraping using a rubber policeman and pelleted by centrifugation. Cell pellet was washed once with PBS and resuspended in 400 μl of gentle lysis buffer (10 mM Tris-HCl at pH 7.5, 10 mM NaCl, 10 mM EDTA, 0.5% TritonX-100, 1 mM phenylmethylsulfonyl fluoride (PMSF), 1× protease inhibitor cocktail [Calbiochem], 1 mM DTT, and 10 μg/ml of RNase A [Roche]) and incubated on ice for 15 minutes. Insoluble materials were removed by centrifugation at 13,400 g in a microcentrifuge at 4°C for 15 minutes. NaCl was added to the cleared lysate to a final concentration of 250 mM, and 350 μl of the lysate incubated with 10 μl of protein A sepharose beads pre-bound with 10 μg of monoclonal anti-Flag M2 antibody at 4°C overnight. The next day, beads were washed and bound fractions eluted with 3× SDS-sample buffer by heating at 95°C for 5 minutes. Proteins were resolved by SDS-polyacrylamide gel electrophoresis (PAGE), followed by Western blot analysis.

RESULTS

Lin28 Knockdown Affects hESC Growth

Both human and mouse ESCs proliferate rapidly and have a unique cell cycle thought to be biologically coupled to pluripotency [19, 20]. This, coupled with the additional evidence discussed above suggesting that Lin28 is involved in stem cell proliferation, led us to ask whether Lin28 might play a direct role in the growth and survival of hESCs. Therefore, we inhibited Lin28 expression using a Lin28-specific siRNA (siLin28) [15, 21]. siLin28 reduced Lin28 expression to 8% and 12% of the control at the RNA (Fig. 1A) and protein (Fig. 1B) level, respectively. Importantly, we observed a concomitant decrease in the number of viable cells (Fig. 1C, left panel) and an increase in apoptosis, which was indicated by an elevated level of caspase 3/7 activity (Fig. 1C, right panel). To rule out possible nonspecific (i.e., off-target) effects of siLin28, we also used another siRNA (siLin28-2; [15]) targeted to a different region of Lin28 mRNA and obtained similar results (Supporting Information Fig. S1). Taken together with our previous findings in mouse ESCs that reducing Lin28 expression slows cell growth and overexpressing Lin28 accelerates cell growth [13], our results support the conclusion that Lin28 is important for the growth and survival of hESCs. We cannot conclude, however, that Lin28 is absolutely essential for hESC viability in vivo. Under our cell culture conditions, we see significant cell death; however, Lin28 knockout mice, though nonviable and weighing less than 20% of wild-type mice at birth [2], suggest that Lin28 deficiency severely compromises cell growth but is not obligatory under all conditions.

Genome-Wide Identification of Lin28 mRNA Targets

How might Lin28 exert its biological effects? Most likely, both let-7-dependent and let-7-independent pathways are involved. To investigate the contribution of mRNA targets that might be regulated by Lin28, we developed a genome-wide approach. Thus, we isolated Lin28-containing RNPs from hESCs by IP, followed by identification of associated
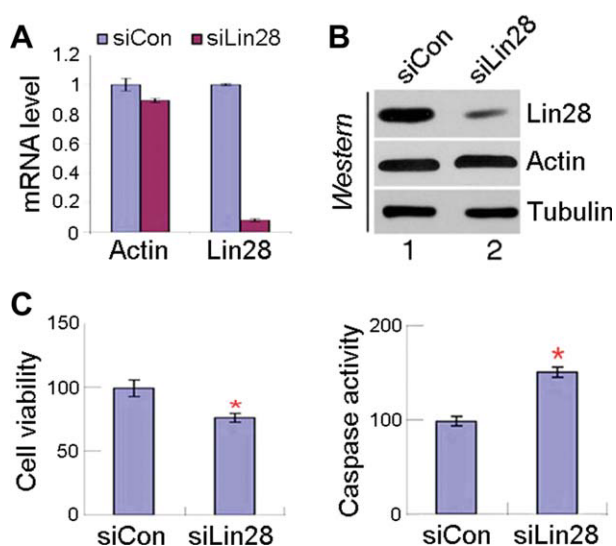
Figure 1. Downregulation of Lin28 reduces the number of viable cells. siLin28 or siCon was transfected into hESC line H1 cells. RNAs and proteins were isolated 72 hours following transfection, and levels measured by RT-qPCR or Western blot analysis. **(A):** Results of RT-qPCR. The levels of β-actin and Lin28 RNAs from control siRNA-transfected cells were set as 1. Error bars are mean ± SD (n = 3). **(B):** Results of Western blot analysis. Antibodies used in Western detection are marked on the right. Protein bands were quantitated using Bio-Rad Quantity One softward. β-tubulin was used as a loading control. **(C):** Cell viability (left panel) and caspase-3/7 activity (right panel) were determined 72 hours post siRNA transfection. Each bar represents mean ± SD (n = 3); *, $p < .01$. Note: The discrepancy between our results and those reported by Darr and Benvenisty [21] showing no detectable effects following Lin28 knockdown in hESCs using the same siRNAs may be caused by different culture conditions used in the two studies, or to different extents of Lin28 reduction that were achieved (88% at the protein level in our study vs. 70% in the other study). Our efficient knockdown of Lin28 expression was the result of a new transfection method as previously reported [15, 22]. Abbreviations: siCon, control siRNA; siLin28, Lin28-specific siRNA.

mRNAs using cDNA synthesis and high throughput deep sequencing with the Illumina platform. The detailed procedures are outlined in "Materials and Methods" and the full list of mRNAs enriched by Lin28 IP is presented in Supporting Information Table S1. Strikingly, we found Lin28 to be highly selective in recognition of mRNAs. Only a small subset (1,259 genes/4.8% of cellular mRNAs) were enriched more than 2.5-fold in the Lin28 IP as compared with the control preimmune IP. We selected the top (lowest p values) 268 genes with at least 2.5-fold enrichment in Lin28 IP versus preimmune IP (Supporting Information Table S2) and carried out GO analysis to classify those mRNA targets into different groups. As shown in Table 1 and Supporting Information Table S3, the top mRNA cluster selected by Lin28 represents genes encoding RNP proteins (including several essential splicing factors), followed by genes participating in translation (including ribosomal proteins and key translation initiation and elongation factors) and genes involved in cellular metabolism. In contrast, many genes are strikingly under-represented in the Lin28 IP samples. Genes relating to membrane receptor activity, DNA-binding and transcription (Oct4 is an exception) are rarely associated preferentially with Lin28. For example, none of the total of 1,271 genes in the human genome that encode G-protein-coupled receptors is among the top 268 selected genes, whereas many ribosomal protein mRNAs are apparent Lin28 targets. We note that most of the

Table 1. GO analysis

N	X	GO attributes	p value	Rank
Overrepresented attributes				
28	841	RNP	<.001	1
45	2,034	Biosynthesis/anabolism	<.001	2
23	703	Structural constituent of ribosome	<.001	3
33	1,304	Macromolecule biosynthesis	.001	4
41	1,842	Cellular biosynthesis	.001	5
31	1,204	Protein biosynthesis	.001	6
87	5,468	Cellular macromolecule metabolism	.001	7
24	831	Mitochondrion	.003	8
4	12	Eukaryotic 48S initiation complex	.003	9
5	26	Cholesterol biosynthesis	.004	10
14	336	Alcohol metabolism	.005	11
11	222	Energy derivation by oxidation of organic compounds/chemicals	.009	12
15	411	Cellular carbohydrate metabolism	.012	13
5	34	Sterol biosynthesis	.012	14
7	91	Glycolysis	.022	15
8	132	Glucose metabolism	.036	16
Underrepresented attributes				
0	1,271	G-protein-coupled receptor activity	.001	1
6	2,463	Zinc binding	.001	2
0	1,075	Rhodopsin-like receptor activity/Class A G-protein-coupled	.007	3
9	2,746	Organismal physiological process	.009	4
2	1,478	G-protein-coupled receptor protein signaling pathway	.015	5
5	1,995	Transmembrane receptor activity	.022	6
17	3,738	Cation binding	.028	7
10	2,742	Transition metal ion binding	.036	8
12	3,026	DNA binding	.036	9

Abbreviations: GO, gene ontology; N, number of genes in the query with this attribute; P, single hypothesis one-sided p value of the association between attribute and query adjusted by fraction of 1,000 null-hypothesis simulations having attributes with this single hypothesis p value or smaller; RNP, ribonucleoprotein particle; X, number of genes overall with this attribute.

genes enriched in the Lin28 IP are consistent with a role of Lin28 in regulating cellular growth and metabolism. Supporting Information Figures S2–S10 show examples of the data obtained.

Our IP and sequencing studies did not involve protein-RNA cross-linking prior to isolation and deep sequencing. We omitted this step for technical reasons as it severely reduced RNA yields, making deep sequencing unreliable. However, several lines of evidence suggest that our target list largely reflects bona fide Lin28 targets. First, in every case, so far, where we have chosen a target from the list for further validation, this has been successful (see below and data not shown). Second, many of the most enriched targets fall into only a few functional categories, as evidenced by our GO analysis (Table 1). Third, Lin28 is clearly not associating preferentially only with the most abundant mRNAs in the extracts. Many highly abundant mRNAs are not enriched at all, whereas a number of moderately abundant and relatively low abundance mRNAs are highly selected.

We selected six genes (representing several different functional categories from the GO analysis) for IP/RT-qPCR validation: CD63 (a transmembrane protein), EEF1G, EIF4A, HMGA1 (a chromosome binding protein), Oct4 (known Lin28 target as a positive control), and RPS13 (a ribosomal protein). β-actin mRNA was a negative control for Lin28 binding. Each of the selected mRNAs was enriched by more than 2.5-fold in the Lin28 IP versus preimmune IP samples from hESCs (Fig. 2A). Similar results were obtained using RNPs isolated from human EC PA-1 cells (Fig. 2B). The ESCs and EC cells share many properties including Lin28 expression, cell surface antigen expression, proliferation characteristics, the ability to self-renew and differentiate, and the

expression of core transcription factors that control their undifferentiated state [23]. Taken together with the GO analysis, we suggest that many or most of the candidate genes selected by our analyses are likely to be in vivo targets of Lin28.

Downregulation of Lin28 Leads to Decreased Levels of Proteins Expressed from Target Genes

If binding to target mRNAs reflects a mode of gene regulation by Lin28 then we would hypothesize that lower Lin28 expression would alter the expression of proteins encoded by these targets. To determine whether Lin28 influences the expression of its target genes, we performed siRNA knockdown experiments. When the level of Lin28 protein in siLin28-transfected cells was reduced to 15% of that seen in siCon transfected cells (Fig. 3A, top panel, compare lane 2 with lane 1), a concomitant decrease in the Oct4 protein level (52% of siCon-transfected cells, second from the top blot, compare lane 2 with lane 1) was also observed. Although this likely results directly from Lin28 interaction with the Oct4 mRNA, it remained possible that the observed effect was indirect, due to changes in hESC growth or pluripotency, or let-7 expression levels resulting from Lin28 knockdown. However, down-regulation of Lin28 also led to decreased protein levels of the other selected target genes, whereas the level of β-actin protein was not affected (Fig. 3A, compare lanes 2 with lanes 1 of the indicated genes). Similar results were obtained when PA-1 cells were used (Fig. 3B). Given that the protein level changes were larger between siLin28 and siCon-transfected cells compared with their respective mRNA level changes, we conclude that the differences between the mRNA and protein level changes observed most likely result from impaired translation due to reduced Lin28 levels.
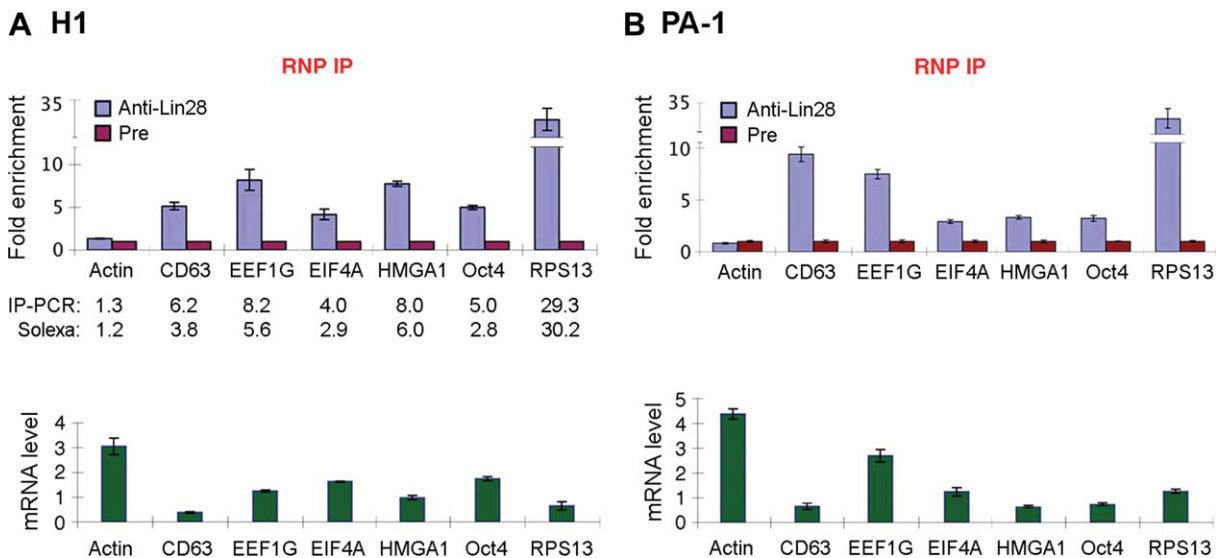
Figure 2. A subset of mRNAs is specifically enriched in Lin28-containing RNPs. RNPs were isolated from undifferentiated hESC H1 (**A**) or PA-1 cells (**B**) using anti-Lin28 antibody or preimmune IgG, followed by RNA extraction and RT-qPCR analyses. Upper panels, relative abundance of the indicated mRNAs associated with anti-Lin28 versus preimmune IP complexes plotted as relative fold enrichment. Bottom panels, relative mRNA levels after normalization against β-tubulin mRNA levels in the cell extracts. Error bars are mean $\pm$ SD ($n = 3$). In (**A**), relative fold enrichment derived from IP/RT-qPCR and deep sequencing (Solexa) analysis are also shown as comparisons. Abbreviations: EEF1G, eukaryotic translation elongation factor 1 gamma; EIF4A, eukaryotic translation initiation factor 4A; HMGA1, high mobility group AT-hook1; IP, immunoprecipitation; PCR, polymerase chain reaction; RNP, ribonucleoprotein particles; RPS13, ribosomal protein S13.

Lin28 Inhibition Induces Shifts of Target mRNAs from Polysomal to Nonpolysomal Fractions

If Lin28 stimulates the translation of target mRNAs, we would expect an enrichment of these mRNAs in polysomes that contain Lin28, whereas nontarget mRNAs such as β-actin would not be enriched. Oct4 mRNA was enriched in Lin28-containing polysomes by greater than threefold, whereas β-actin mRNA was not enriched at all (Supporting Information Fig. S11A and [15]). Similarly, EEF1G, HMGA1, and RPS13 mRNAs were also enriched at least twofold in Lin28-containing polysomes (Supporting Information Fig. S11A). Importantly, the fold enrichments observed did not reflect the steady-state levels of the respective mRNAs in the polysomes (Supporting Information Fig. S11B), indicating that association of these mRNAs with Lin28 in polysomes is specific and that Lin28 likely plays a role in modulating the translation of these mRNAs.

As in most cases an increased polysome association of an mRNA indicates an increase in translation efficiency, we next asked whether downregulation of Lin28 would shift target mRNAs from polysomes to nonpolysome fractions. Thus, PA-1 cells were transfected with siLin28 or siCon, followed by sucrose gradient fractionation of cytoplasmic extracts collected 48 hours after transfection. Total RNAs were isolated from polysome or nonpolysome fractions (which included RNP, 40S, 60S, and 80S fractions), and polysome distributions of indicated mRNAs analyzed. We observed significant decreases in polysome association of the putative target mRNAs in siLin28-transfected cells versus siCon-transfected cells. The decreases were 65%, 40%, 85%, and 56% with EEF1G, HMGA1, Oct4, and RPS13 mRNAs, respectively, whereas polysome association of β-actin mRNA decreased by only 13% (Fig. 3C, top panel). Given that the steady-state mRNA levels were essentially unchanged (Fig. 3C, bottom panel), we conclude that the decreased polysome association of the target mRNAs was most likely due to reduced translation.

Target Genes Contain LREs in Their Coding Regions

We have previously mapped a 369-nt long LRE within the coding region of Oct4 mRNA (called Oct4-R2) that allows for Lin28-dependent stimulation of translation in a reporter system [15]. To determine whether EEF1G, HMGA1, and RPS13 mRNAs also contain LREs, we initiated mapping using a luciferase reporter [15]. As an additional positive control for luciferase stimulation, we included a 393-nt-long fragment derived from the ORF of the mouse histone H2a gene shown to stimulate the translation in a Lin28-dependent fashion [14]. As a negative control, we used Oct4-R4, a fragment derived from the Oct4 3′UTR [15]. We identified LREs in all three genes, all of which mapped to the coding regions (Fig. 4A). We next assessed the activity of shorter derivatives of the Oct4-R2 element. We obtained a 95-nt-long sequence that retains the full activity of the 369-nt-long R2 fragment (Fig. 4A, 4B). However, further deletion of either end of the fragment completely abolished activity (Fig. 4B). In similar experiments using elements derived from HMGA1, RPS13, and EEF1G, we have likewise been unable to identify any LRE shorter than 95-nt, consistent with an idea that Lin28 recognition may involve RNA structural features rather than simple sequence motifs.

RHA Participates in Lin28-Dependent Stimulation of Translation

Lin28 interacts specifically with RHA and downregulation of RHA expression impedes Lin28-dependent stimulation of translation in a reporter system [15]. The Lin28 protein contains two types of RNA-binding motifs: a cold shock domain (CSD) and a pair of retroviral-type cys-cys-his-cys (CCHC) zinc fingers (Fig. 5D) [24, 25]. Inactivation by point mutations of either CSD or CCHC domain led to the loss of the ability of Lin28 to associate with mRNA [26]. These same mutations do not affect its interaction with RHA (data not
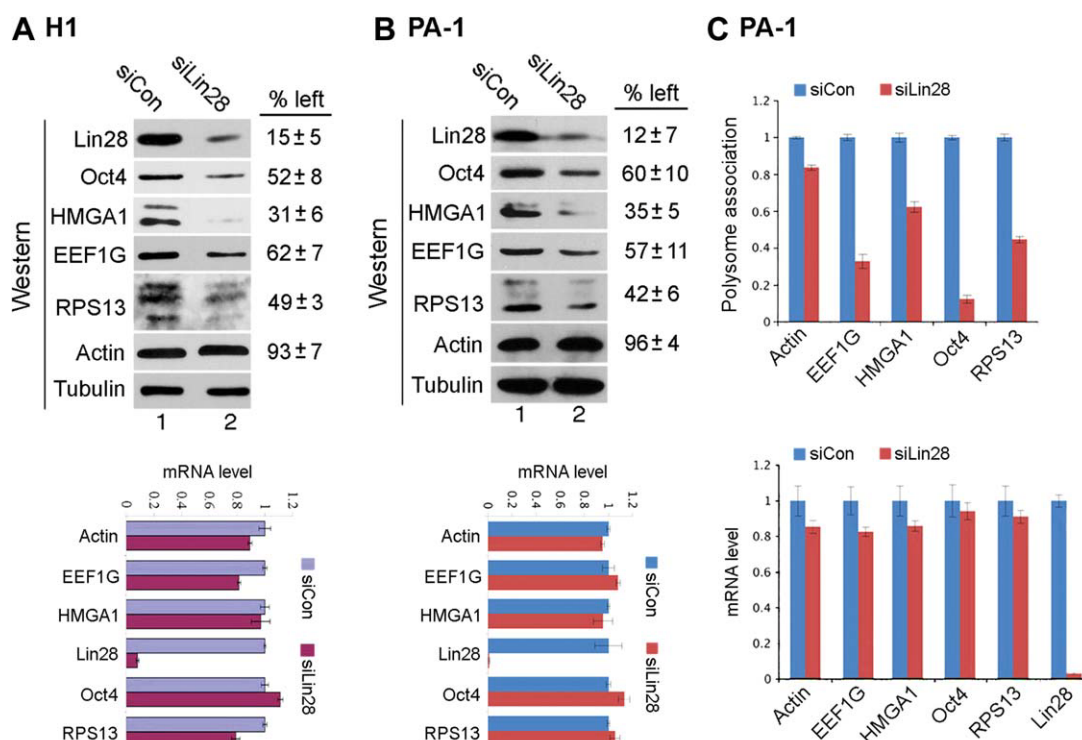
Figure 3. Downregulation of Lin28 leads to decreased protein expression from target genes. H1 (**A**) or PA-1 (**B**) cells were transfected with siCon or siLin28. Protein and RNA were extracted 72 hours later and levels measured by Western blot and RT-qPCR. Representative results of three independent transfections for each cell type are shown. Levels of the indicated proteins in siLin28- versus siCon-transfected cells (set as 100%) are on the right. Protein levels were determined using Bio-Rad Quantity One software, and calculated after normalization against β-tubulin loading control. Numbers are mean $\pm$ SD ($n = 3$). Bottom panels, relative mRNA levels after normalization against β-tubulin control. mRNA levels in cells transfected with siCon were arbitrarily set as 1. Numbers are mean $\pm$ SD ($n = 3$). (**C**): PA-1 cells were transfected with siCon or siLin28. Polysome fractionation was carried out 48 hours post-transfection. Upper panel, RNAs were extracted from each fraction (RNP, 40S, 60S, 80S, and polysomes) and subjected to RT-qPCR using primers specific for the indicated genes. The efficiency of translation was then calculated, after normalization to β-tubulin mRNA, by comparing the RNA level in polysomes with total fractions (combining the polysome and nonpolysome fractions). Polysome association of mRNAs in siCon-transfected cells were arbitrarily set as 1. Numbers are mean $\pm$ SD ($n = 3$); p, < .01. Bottom panel, total RNAs were extracted from cells transfected with siCon or siLin28 48 hours post-transfection. Levels were measured by RT-qPCR. RNA levels from siCon-transfected cells were arbitrarily set as 1. Numbers are mean $\pm$ SD ($n = 3$). Abbreviations: EEF1G, eukaryotic translation elongation factor 1 gamma; HMGA1, high mobility group AT-hook1; RPS13, ribosomal protein S13; siCon, control siRNA; siLin28, Lin28-specific siRNA.

shown). However, a 35-aa deletion at the carboxyl terminus of Lin28 dramatically diminishes its ability to interact with RHA (Fig. 5A, 5D) but not RNA (Supporting Information Fig. S12C). As shown in Figure 5A, while approximately 4% of endogenous RHA was coimmunoprecipitated with the wild-type Flag-Lin28, only ~0.3% of RHA was precipitated with the mutant Lin28 (top panel, compare lane 2 with lane 1). Importantly, the mutant Lin28 not only reduced its ability to stimulate translation (Supporting Information Fig. S12A, S12B), but also exhibits an inhibitory effect in the presence of wild-type Lin28 (Fig. 5B, top panel), whereas the expression levels of RHA and Flag-Lin28 were not altered as a result of the mutant expression (Fig. 5B, bottom panel). When the mutant Lin28 was expressed in PA-1 cells, we expectedly observed an inhibition of translation of the endogenous target mRNAs as judged by the polysome shift analysis. In the presence of Flag-Lin28ΔC expression, the association of EEF1G, HMGA1, Oct4, and RPS13 mRNAs with polysomes decreased by 81%, 42%, 40%, and 43%, respectively, compared with those in empty vector transfected cells (Fig. 5C and Supporting Information Fig. S13A). Importantly, Flag-Lin28ΔC expression also leads to decreased cell viability (Supporting Information Fig. S13B), consistent with decreased translation of mRNAs important for cell growth and survival.

Taken together, these results thus suggest that Lin28-mediated translational stimulation occurs through the concerted interaction and activities of two RNA-binding proteins.

DISCUSSION

A major biological function of Lin28 is to support the rapid growth of ESCs. This is supported by the following evidences: (a) during reprogramming, Lin28 increases the number of human iPSC colonies, consistent with its ability to promote the proliferation and survival of reprogrammed cells [1]; (b) in mouse ESCs inhibition of Lin28 slows cell proliferation, whereas overexpression of Lin28 accelerates cell proliferation [13]; (c) in transgenic mice, overexpression of Lin28 leads to increased cell proliferation [2]; and (d) downregulation of Lin28 in hESCs or expression of a mutant Lin28 that is incapable of RHA interaction in PA-1 cells results in decreased numbers of viable cells, likely a combined result of decreased cell proliferation and survival (this report).

We have used IP and deep sequencing to identify Lin28 target mRNAs and show that Lin28 selectively enriches mRNAs from several distinct classes. The high selectivity of
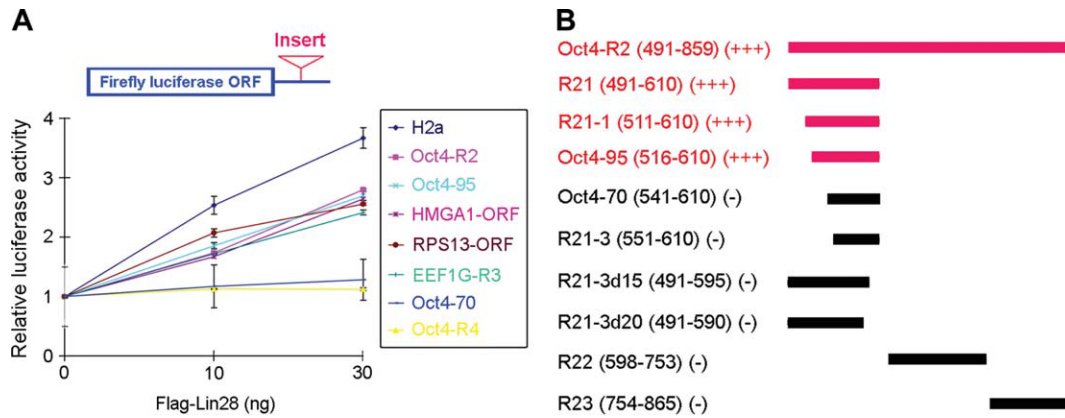
Figure 4. Target genes contain Lin28-responsive elements in their coding regions. **(A):** Luciferase assays. Shown on top is a schematic drawing of the firefly luciferase reporter. The blue box represents ORF, and the blue line represents 3′UTR. The sizes (in nucleotides, relative to transcriptional start sites) for the H2a, Oct4-R2, Oct4-95, HMGA1-ORF, RPS13-ORF, EEF1G-R3, and Oct4-70 fragments inserted at the luciferase 3′UTR are 393 (nt 49–441), 369 (nt 491–859), 217 (nt 1,138–1,354), 95 (nt 516–610), 291 (nt 323–613), 456 (nt 33–488), 330 (nt 811–1,140), and 70 (nt 541-610), respectively. The reporter constructs were each transfected into HEK293 cells, together with increasing amounts of Flag-Lin28. Luciferase activities and mRNA levels were measured 24 hours post-transfection. Relative firefly luciferase activities were plotted after normalization against firefly luciferase mRNA levels. Firefly luciferase activities from cells without Flag-Lin28 transfected were arbitrarily set as 1. Numbers are mean ± SD ($n = 3$). **(B):** Schematics of the minimal Lin28-responsive element mapping of Oct4-R2 using luciferase reporter assays. +++, luciferase activity is 90%–100% of that of Oct4-R2; −, luciferase activity less than 20% of that of Oct4-R2. Abbreviations: EEF1G, eukaryotic translation elongation factor 1 gamma; HMGA1, high mobility group AT-hook1; ORF, open reading frame; RPS13, ribosomal protein S13.
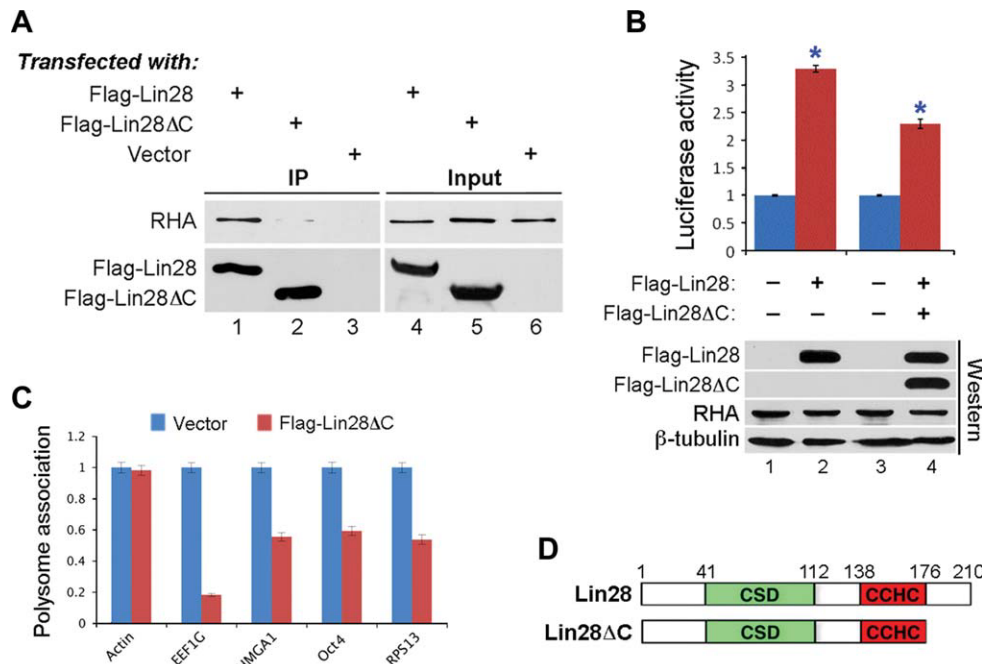
Figure 5. A C-terminal deletion mutant of Lin28 has a dominant-negative effect on Lin28-dependent stimulation of translation. **(A):** Flag-Lin28 (lanes 1 and 4) or Flag-Lin28ΔC (lanes 2 and 5) was transfected into HEK293 cells. Co-IP was carried out 48 hours later using a monoclonal anti-Flag M2 antibody. Co-IP using lysate from vector-transfected cells (lanes 3 and 6) was carried out in parallel as a negative control for nonspecific binding. The resulting co-IP samples were resolved by SDS-PAGE, followed by Western Blot analysis. Antibodies used in the Western blot analysis were anti-RHA (top blots) and a polyclonal anti-Flag (bottom blots). In lanes 4–6, 3% of input was loaded. Bands on Western gels were quantitated using Bio-Rad Quantity One software. **(B):** HEK293 cells were transfected with Oct4-95, with (+) or without (−) cotransfection of Flag-Lin28 (50 ng) and/or Flag-Lin28ΔC (50 ng). Luciferase assays were performed 24 hours later. Top panel, results of luciferase activities, with those in the absence of Flag-Lin28 expression set as 1. Numbers are mean ± SD ($n = 3$); *, $p < .01$. Bottom panel, Western blot analysis showing expression levels of the indicated proteins from transfected cells. β-tubulin was used as a loading control. Bands on Western gels were quantitated using Bio-Rad Quantity One software. **(C):** PA-1 cells were transfected with Flag-Lin28ΔC or empty vector. Polysome fractionation was carried out 48 hours post-transfection. RNAs were extracted from each fraction (RNP, 40S, 60S, 80S, and polysomes) and subjected to RT-qPCR using primers specific for the indicated genes. The efficiency of translation was calculated as described in Figure 3C. Polysome association of mRNAs in empty vector transfected cells were set as 1. Numbers are mean ± SD ($n = 3$); $p, < .01$. **(D):** Schematic representations of wild-type and mutant Lin28 protein. The CSD and CCHC domains are marked. The numbers are in amino acids. Figure not drawn to scale. Abbreviations: CCHC, cys-cys-his-cys; CSD, cold shock domain; EEF1G, eukaryotic translation elongation factor 1 gamma; HMGA1, high mobility group AT-hook1; IP, immunoprecipitation; RHA, RNA helicase A; RPS13, ribosomal protein S13.

Lin28 for ribosomal protein mRNAs (Table 1 and Supporting Information Table S2) is striking and fits well with a role for this protein in growth stimulation, as rapid ESC growth requires coordinated production of ribosomes. Ribosome biogenesis is connected to cell cycle control [27], and its perturbation can lead to cell cycle arrest and/or apoptosis [28, 29]. Many but not all ribosomal protein mRNAs are selected by Lin28 (Table 1 and Supporting Information Tables S1–S3). This may reflect the fact that ribosomal mRNA expression is regulated by both common and distinct mechanisms, depending on the cell type and environmental conditions [30]. Lin28 also selects mRNAs that encode proteins involved in metabolism (Table 1 and Supporting Information Table S2). Not coincidentally, Zhu et al. [2] observed that transgenic mice overexpressing Lin28 not only grew bigger but also manifested increased glucose metabolism. A direct stimulation of translation of the related mRNA targets by Lin28 could well be the basis for many of the effects observed, especially in tissues and cells where let-7 expression was not affected [2]. It is important to note that a fraction of the mRNA targets we have identified may also be regulated by let-7. Experiments using mutant forms of Lin28 and/or let-7 microRNAs that allow the uncoupling of the two activities (i.e., translational stimulation vs. inhibition of let-7 processing) are underway to address this issue.

Lin28 most likely exerts its biological effects by binding to its RNA targets. However, how this protein recognizes RNA is still unclear. Although Lin28 has been reported to affect let-7 processing at a variety of steps, the mechanism(s) by which Lin28 does this are still somewhat controversial and key RNA-protein interactions likely involve not only specific sequence motifs but also structural elements [3, 5, 6]. It is also clear that the reported Lin28 binding elements show only relatively low or modest affinities for the protein in vitro [3, 5]. We show here that most Lin28 mRNA targets so far examined (including Oct4, RPS13, HMGA1, EEF1G, and histone H2a) contain LREs in their coding regions (Fig. 4; [14]). Coding regions are the sequences expected to be most highly conserved between human and mouse. In addition, our sequence mapping studies suggest that Lin28 is not recognizing short sequence motifs (Fig. 4). Thus, although we initially hoped to find that Lin28 binds to short sequence motifs like many other RNA binding proteins (such as SR proteins [31] and Nova [32]), results have revealed that this is not likely to be the case. Our current hypothesis is that Lin28 recognizes its targets either (a) along with one or more additional cellular factors and/or (b) via binding to larger structured regions of RNA. This second model is consistent with the mechanism by which Lin28 affects let-7 processing [3, 5–7, 33]. Also, there are a number of RNA-binding proteins that recognize only longer RNA sequences/structures. These include the human immunodeficiency virus (HIV-1) Rev protein [34], the essential mRNA export factor NXF1 [35], and RHA [36, 37].

Finally, we note from our GO analysis that there are several additional and possibly quite important classes of Lin28 targets. A number of chromosomal proteins (such as HMGA1 and chromatin modifying protein 2A (CHMP2A); see Supporting Information Table S2) may be regulated by Lin28 and these may participate in the establishment or maintenance of the unique chromatin structure found in pluripotent cells. Importantly, knockdown of Lin28 leads to lower levels of HMGA1 protein in both hESCs and in PA-1 cells (Fig. 3). Also, another enriched class of Lin28 targets include mRNAs encoding RNA-binding proteins, such as a number of proteins involved in pre-mRNA splicing or RNA metabolism (such as poly(U)-binding-splicing factor 60 (PUF60), mago nashi homolog (MAGOH), ras-related nuclear protein (RAN) and the arginine methyltransferases protein arginine methyltransferase 1 (PRMT1) and PRMT2; see Supporting Information Table S2). It will be interesting to investigate alterations in alternative splicing patterns, mRNA trafficking and turnover in response to either upregulation or downregulation of Lin28 expression.

CONCLUSION

Our genome-wide studies show that Lin28 associates preferentially with a relatively small subset of cellular messages. These targets primarily fall into several functional classes, most of which represent genes that are important for cell growth and survival. We also find that Lin28 recognizes specific sequence elements within its target mRNAs and, in concert with RNA helicase A, enhances the translation of these mRNAs into proteins. These findings open new avenues of future work on the role of Lin28 in pluripotency and stem cell function.

ACKNOWLEDGMENTS

DISCLOSURE OF POTENTIAL CONFLICTS OF INTEREST

The authors indicate no potential conflicts of interest. The contents of this material are solely the responsibility of the authors and do not necessarily represent the official views of the State of Connecticut, the Department of Public Health of the State of Connecticut, or Connecticut Innovations, Incorporated.

REFERENCES

1 Yu J, Vodyanik MA, Smuga-Otto K et al. Induced pluripotent stem cell lines derived from human somatic cells. Science 2007;318: 1917–1920.

2 Zhu H, Shah S, Shyh-Chang N et al. Lin28a transgenic mice manifest size and puberty phenotypes identified in human genetic association studies. Nat Genet 2010;42:626–630.

3 Viswanathan SR, Daley GQ, Gregory RI. Selective blockade of MicroRNA processing by Lin-28. Science 2008;320:97–100.

4 Roush S, Slack FJ. The let-7 family of microRNAs. Trends Cell Biol 2008;18:505–516.

5 Newman MA, Thomson JM, Hammond SM. Lin-28 interaction with the Let-7 precursor loop mediates regulated microRNA processing. RNA 2008;14:1539–1549.

6 Piskounova E, Viswanathan SR, Janas M et al. Determinants of micro-RNA processing inhibition by the developmentally regulated RNA-binding protein Lin28. J Biol Chem 2008;283:21310–21314.

7 Trabucchi M, Briata P, Garcia-Mayoral M et al. The RNA-binding protein KSRP promotes the biogenesis of a subset of microRNAs. Nature 2009;459:1010–1014.

8 Heo I, Joo C, Cho J et al. Lin28 mediates the terminal uridylation of let-7 precursor MicroRNA. Mol Cell 2008;32:276–284.

9 Hagan JP, Piskounova E, Gregory RI. Lin28 recruits the TUTase Zcchc11 to inhibit let-7 maturation in mouse embryonic stem cells. Nat Struct Mol Biol 2009;16:1021–1025.

10 Lehrbach NJ, Armisen J, Lightfoot HL et al. LIN-28 and the poly(U) polymerase PUP-2 regulate let-7 microRNA processing in *Caenorhabditis elegans*. Nat Struct Mol Biol 2009;16:1016–1020.

11 Balzer E, Heine C, Jiang Q et al. LIN28 alters cell fate succession and acts independently of the let-7 microRNA during neurogliogenesis in vitro. Development 2010;137:891–900.

12 Polesskaya A, Cuvellier S, Naguibneva I et al. Lin-28 binds IGF-2 mRNA and participates in skeletal myogenesis by increasing translation efficiency. Genes Dev 2007;21:1125–1138.

13 Xu B, Zhang K, Huang Y. Lin28 modulates cell growth and associates with a subset of cell cycle regulator mRNAs in mouse embryonic stem cells. RNA 2009;15:357–361.

14 Xu B, Huang Y. Histone H2a mRNA interacts with Lin28 and contains a Lin28-dependent posttranscriptional regulatory element. Nucleic Acids Res 2009;37:4256–4263.

15 Qiu C, Ma Y, Wang J et al. Lin28-mediated post-transcriptional regulation of Oct4 expression in human embryonic stem cells. Nucleic Acids Res 2010;38:1240–1248.

16 Langmead B, Trapnell C, Pop M et al. Ultrafast and memory-efficient alignment of short DNA sequences to the human genome. Genome Biol 2009;10:R25 doi: 10.1186/gb-2009-10-3-r25.

17 Mortazavi A, Williams BA, McCue K et al. Mapping and quantifying mammalian transcriptomes by RNA-Seq. Nat Methods 2008;5:621–628.

18 Berriz GF, Beaver JE, Cenik C et al. Next generation software for functional trend analysis. Bioinformatics 2009;25:3043–3044.

19 Becker KA, Stein JL, Lian JB et al. Human embryonic stem cells are pre-mitotically committed to self-renewal and acquire a lengthened G1 phase upon lineage programming. J Cell Physiol 2010;222:103–110.

20 White J, Dalton S. Cell cycle control of embryonic stem cells. Stem Cell Rev 2005;1:131–138.

21 Darr H, Benvenisty N. Genetic analysis of the role of the reprogramming gene LIN-28 in human embryonic stem cells. Stem Cells 2009;27:352–362.

22 Ma Y, Jin J, Dong C, Cheng E-C, Lin H, Huang Y, Qiu C. High-efficiency siRNA-based gene knockdown in human embryonic stem cells. RNA 2010;16:2564–2569.

23 Greber B, Lehrach H, Adjaye J. Silencing of core transcription factors in human EC cells highlights the importance of autocrine FGF signaling for self-renewal. BMC Dev Biol 2007;7:46 doi: 10.1186/1471-213X-7-46.

24 Moss EG, Lee RC, Ambros V. The cold shock domain protein LIN-28 controls developmental timing in *C. elegans* and is regulated by the lin-4 RNA. Cell 1997;88:637–646.

25 Moss EG, Tang L. Conservation of the heterochronic regulator Lin-28, its developmental expression and microRNA complementary sites. Dev Biol 2003;258:432–442.

26 Balzer E, Moss EG. Localization of the developmental timing regulator Lin28 to mRNP complexes, P-bodies and stress granules. RNA Biol 2007;4:16–25.

27 Lempiainen H, Shore D. Growth control and ribosome biogenesis. Curr Opin Cell Biol 2009;21:855–863.

28 Chen D, Zhang Z, Li M et al. Ribosomal protein S7 as a novel modulator of p53-MDM2 interaction: Binding to MDM2, stabilization of p53 protein, and activation of p53 function. Oncogene 2007;26:5029–5037.

29 Zhang Y, Wolf GW, Bhat K et al. Ribosomal protein L11 negatively regulates oncoprotein MDM2 and mediates a p53-dependent ribosomal-stress checkpoint pathway. Mol Cell Biol 2003;23:8902–8912.

30 Hamilton TL, Stoneley M, Spriggs KA et al. TOPs and their regulation. Biochem Soc Trans 2006;34:12–16.

31 Huang Y, Steitz JA. SRprises along a messenger's journey. Mol Cell 2005;17:613–615.

32 Ule J, Jensen K, Mele A et al. CLIP: A method for identifying protein-RNA interaction sites in living cells. Methods 2005;37:376–386.

33 Heo I, Joo C, Kim YK et al. TUT4 in concert with Lin28 suppresses microRNA biogenesis through pre-microRNA uridylation. Cell 2009;138:696–708.

34 Lesnik EA, Sampath R, Ecker DJ. Rev response elements (RRE) in lentiviruses: An RNAMotif algorithm-based strategy for RRE prediction. Med Res Rev 2002;22:617–636.

35 Li Y, Bor YC, Misawa Y et al. An intron with a constitutive transport element is retained in a Tap messenger RNA. Nature 2006;443:234–237.

36 Hartman TR, Qian S, Bolinger C et al. RNA helicase A is necessary for translation of selected messenger RNAs. Nat Struct Mol Biol 2006;13:509–516.

37 Roberts TM, Boris-Lawrie K. Primary sequence and secondary structure motifs in spleen necrosis virus RU5 confer translational utilization of unspliced human immunodeficiency virus type 1 reporter RNA. J Virol 2003;77:11973–11984.

See www.StemCells.com for supporting information available online.